IASJ المجلات الاكاديمية العراقية

Tikrit Journal of Pure Science

ISSN: 1813 – 1662 (Print) --- E-ISSN: 2415 – 1726 (Online)

Journal Homepage: http://tjps.tu.edu.iq/index.php/j

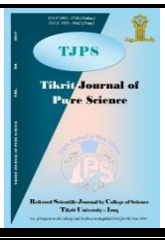

Integrating GIS-based and geophysical techniques for groundwater potential assessment in Halabja Said Sadiq sub-basin, Kurdistan, NE Iraq

Hawber A. Karim, Diary A. Al-Manmi

College of Science, University of Sulaimani, Sulaymaniyah, Iraq

https://doi.org/10.25130/tjps.v24i6.441

ARTICLE INFO.

Article history:

-Received: 26 / 5 / 2019

-Accepted: 26 / 6 / 2019

-Available online: / / 2019

Keywords: Groundwater productivity, AHP, geoelectric resistivity, Kurdistan

Corresponding Author:

Name: Hawber A. Karim

E-mail:

hawberatakarem@gmail.com

Tel: +9647701492772

ABSTRACT

Groundwater is an important resource in Halabja Said Sadiq sab-basin, Sulaymaniyah district for agricultural and other uses. Continuous dramatic extraction of groundwater from legal and illegal wells led to a severe decline in the water table for the last thirty years. The objectives of this study are to delineate the groundwater productivity zones by combining the geographic information system and geoelectrical survey, which serves to recognize the locations of good groundwater storage and recharge zones. The Halabja Said Sadiq sub-basin has been selected as a case study to delineate the groundwater productivity zones. Four geoelectrical resistivity profiles conducted with electrode spacing 10 m and the length of the profiles is equal to 710 m. Themes such as hydrogeology, land use/land cover, topography, drainage density, soil type, slope, lineaments and rainfall maps are created. The thematic maps made with GIS platform and appropriate weights put to the attributes taking into account the influence on the storage potential of groundwater. The results of geoelectrical profiles revealed that the aquifer thickness is 150 m. Three zones of groundwater potential delineated which are low, moderate and high and cover 33 %, 24 %, and 42 % of the total area respectively. Spatially, the highest zone is located along with the Quaternary deposits which characterized by high lineament density, low slop, and pediment deposition

The output of the groundwater potential model is verified by testing the discharge rate of the existing 580 wells. The results are revealed that most of the high yield wells are located within the high groundwater potential zone. Results of such verifications proved that the groundwater productivity areas recognized by GIS (AHP) and geoelectrical techniques are dependable and practical.

Introduction

Rapid population growth ،urbanization, agricultural, and industrial activities in Kurdistan region led to increased demand for fresh water to meet the expanding needs. Groundwater considers being a significant water supply in some regions because it is fresh water and not polluted. The study area considers as one of the most fertile plains in Iraq with certain annual rainfall for cropping and a large reserve of groundwater. The groundwater existence often depends on factors such as geology, climate, hydrogeology, topography and structural geology [1]. The data about groundwater can be achieved through remote sensing and topographical data with truth ground data [2].

The term groundwater potential means the quantity of groundwater available in a specific area and it is a function of various hydrologic and hydrogeologic circumstances [3]. From a hydrogeological investigation aspect, it can be defined as the possibility of groundwater occurring in an area. Appropriate assessment of groundwater potential can help as useful guidelines for the decision maker in recognizing suitable groundwater policies within an area and appropriate management of the aquifer system in a sustainable method. Maps of potential mappings also used in the selection of suitable well-sites and thus help effective planning of groundwater [4]; [5].

The first attempt of groundwater investigation using remote sensing and GIS techniques was [6]. He developed a unique methodology for integrating multiple data to identify groundwater and locating water wells. [7];[8]; [9], stated that the GIS method is a powerful tool for the combination and analysis of many thematic layers in delineating groundwater potential areas. [10] showed the capability of remote sensing and GIS techniques for demarcating groundwater potential zones. Nevertheless, some researchers like [11]; [12]; [13]; [14]; [1]; [15]; [16] ;[17]. successfully have integrated GIS and geophysical approaches for groundwater potential mapping studies.The type and number of factors used for evaluating groundwater potential differ significantly from one study to another reliant on the accessibility of data in an area and frequently their selection is arbitrary. Also, in a majority of the studies concerning the delineation of groundwater potentiality, personal judgment and dexterity opinion play a major role in thematic layers selection [18].

Geoelectrical resistivity method is the most widespread and cost-effective of all the geophysical methods for groundwater prospecting [16]. The method has made a lot of phenomenal progress in its utilization over the past decades. The geoelectrical resistivity method is the most widespread and cost-effective of all the geophysical methods for groundwater prospecting [16]. The method has developed remarkable progress in its utilization over the past years. The basic principles of this method are depending on the electrical resistivity of the components of geological formations in addition to porosity and water content of the formation [19]. However it is used frequently to determine aquifer's structure, yet there is a substantial interest in the opportunities of determining aquifer characteristics such as permeability and porosity from the measurements of geophysical properties [20] ;[21].

Remote sensing, GIS and geoelectrical resistivity methods were proved good results for delineation groundwater potential zones when matched to observed productivity data [22];[14]. Satellite IRS-IC LISS III, Landsat TM digital and SRTM data are used by [23] to prepare various topical maps. [24] concentrated on the description for groundwater change with the aid of remote sensing. [25] used remote sensing and geological data frame into one of the heading methods in the field of groundwater investigation, which assists in surveying, monitoring, and controlling groundwater assets.

The objective of this study to delineate groundwater potential zones for the assessment of groundwater availability in the study basin using an integration of geoelectrical resistivity and GIS techniques.

Location of the Study area

The Halabja Saidsadiq basin is situated to the southeastern of Sulaimani Governorate in the northeastern of Iraq. Geographically it is located between the latitude N35^0 03′ 39.40″ and N35^0 35′ 51.50″ and the longitude E45^0 32′ 24.70″ and E 46^0 12′ 51.60″ (Fig.1). The basin coverage area is about 1544 km^2, and the elevation range from 453-2500 m above mean sea level, with a population of about 190,727 persons in 2015 in accordance with the data achieved from Sulaimani Statistical Directorate. In the study basin, groundwater performs an important role in supplying water for drinking, industrials and agricultural activities. The climate of the area is characterized by wet in winter and dry in summer and the average annual precipitation in the area ranging from 500 to 700 mm for long period [14].

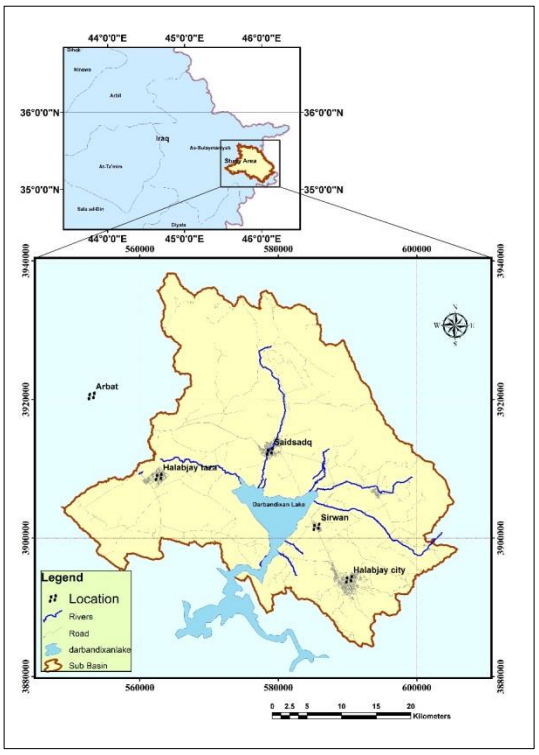

Fig. 1: Location map of the study area

Geology and Hydrogeology of study area.

According to the tectonic classification of [26] and [27], the study area is mostly in the High Folded Zone and partially in the Thrust and Imbricated Zones. The region is a portion of the Western Zagros Fold-Thrust Belts. The age of the rocks is ranged from Jurassic to recent. According to [28] the old exposed rocks in the basin starting from the Jurassic age of Sarki, Sehkanian, Barsarin, Naokelekan, and Sargalu Formations (Fig.2). The Thrust Zone includes, Qulqula Radiolarian Formation (Tithonian – Albian), Qulqula Conglomerate Formation (Cenomanian) and Avroman Group are located directly to the north and northeast of the studied basin. Kometan (Turonian) and Balambo (Valanginian - Cenomanian) Formations the upper Cretaceous and lower Cretaceous are spread in north-west and south-east, Tanjero (upper Senonian) locate in the south-west. The Tertiary formation includes Kolosh (Palaeocene-Eocene), Gercus (middle Eocene), Pilaspi (middle and upper Eocene), Fatha

(middle Miocene) generally located in the south of basin near Derbandikhan lake. Quaternary deposits are the essential unit regarding hydrogeological characteristics and water availability. The types of sediments are channel margin, over bank deposits, and channel deposits [29].

There are four aquifer systems in the study area as a result of the presence of different geological formations. The highest water table is recorded in the northern part of the basin, while the central and the southeastern part is characterized by a shallow water table. The general groundwater flow direction is from elevated mountain areas toward lower elevation to the reservoir of Derbandikhan Dam [29].

Materials and methods

1.The geoelectrical resistivity data acquisition

For the 2D geoelectrical survey, four sites have been chosen using the SYSCAL R1 Plus resistivity meter (Fig.3). The electrode spacing for each survey was operated with 10m using the Wenner array method. The length of each traverse is 710 m with 72 electrodes using Multi-Core Spread Cable, for every single site 682 reading data collected. The Wenner array gives an outstanding signal-noise ratio with the other arrangements which is inversely related to the geometric factor. The Wenner geometric factor gives a smaller value than the geometric factor of other configurations [30]; [31]. For the analyzing and processing the obtained data RES2DINV software is used ([32]; [33]) software. The raw resistivity data were treated from three to four repetitions as it shows more logic subsurface geologically with comparatively smaller RMS error.

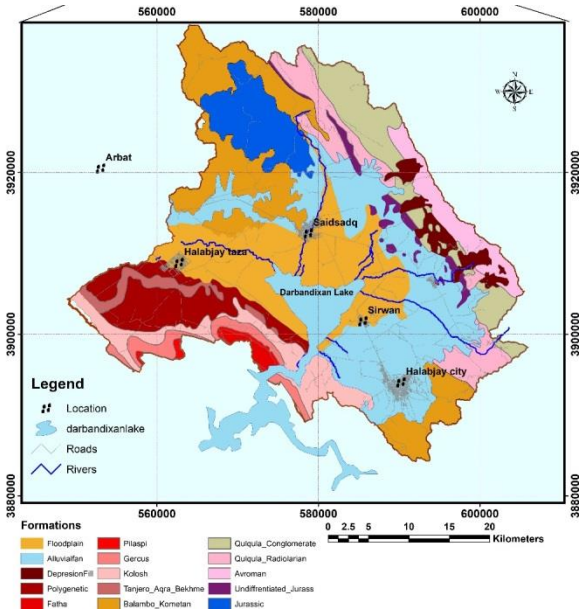

Fig. 2: geology of the study area[27]

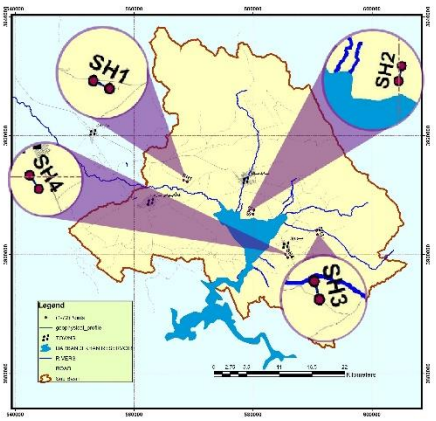

Fig. 3: Location map showing the geoelectric survey profile

Groundwater potential mapping based on AHP technique

For groundwater potential mapping based on the AHP technique, the methodology and data gathering consist of two phases. The first phase was collecting appropriate information from the previous studies and identification of the controlling factors of groundwater recharge. Furthermore, complete data of the study area is gathered on hydrogeology, soils, geology, lithology, structural features, and wells data in the area. The second phase eight thematic layers are integrated which are a hydrogeological map, soil, rainfall data, drainage density and lineaments maps as well as remotely sensed data of land use- land cover, topography, and slope.

The geological map of the area is prepared by compiling Iraqi geological survey maps and then it drives to the hydrological map. The detailed procedure of groundwater potential mapping is shown in Fig.4.

The soil map of FAO (2002) is digitized for preparing the soil layer of the area of interest.

Remote sensing data, Arc GIS 10.5 software, and PCI Geomatica 2016 are used for the preparation of the thematic maps. Land cover was made using Satellite image Landsat 8, July 2018 TM 30m, in addition for the mean annual rainfall distribution International satellite GPM is used. In the present study, the analytical hierarchical process (AHP) method is used which proposed by [34]. This method gives a flexible and quickly learned the way of investigation to complex problems. A nominal system is used to allow the decision maker to include personal experience and knowledge intuitively and easily [35]; [36]; [37]. The thematic layers were reclassified and mapped using the AHP method in a GIS environment to delineate the groundwater potential zones.

Consistency ratios for all thematic maps and their attributes of the assigned weights are determined and it was less than 10 % and by this means implying that the assigned weights are compatible [38]. The eight thematic layers were arranged according to their relevant importance in controlling groundwater

potential [39]; [14]; [40]. The pair-wise comparison was determined for all eight layers, and the reclassified map of them created based on the weights measured (Table 1).

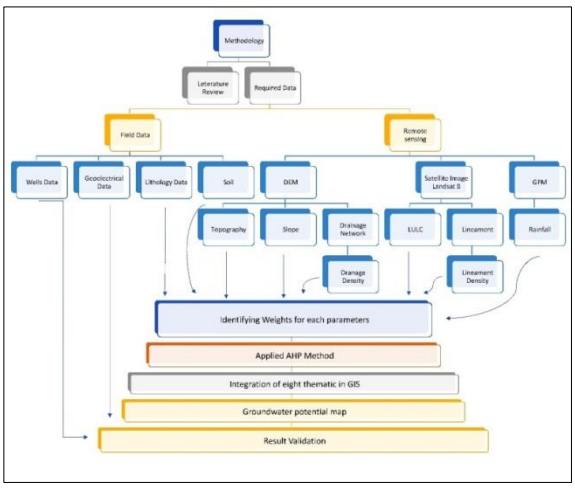

Fig. 4: Flow chart showing AHP method for groundwater potential mapping

Thematic layers of groundwater potential map

1. Hydrogeological Map

Hydrogeology is the essential factor influence on groundwater accumulation and determining the potential of the area, primary porosity and permeability of rocks lithology and thickness, effects weather unit have higher groundwater storage and higher groundwater yields or not. There are four hydrogeological units in the study area (Fig.5 a). Each geological unit is leading to be arranged in one of those hydrogeological aquifers which are intergranular, fissured, karstic aquifers, and aquitard [29]; [41]. The weight is ranked from higher potential to lower potential of groundwater accumulation respectively.

2. Drainage density map

Drainage density influence indirectly on the suitability of groundwater assemblage, because of its connection with infiltration capacity and permeability. The greater the drainage density decreased the infiltration of water to the groundwater zones, which in turn leads to higher runoff and vice versa. When the drainage system of the area compared with the structure it seems that it is controlled by the typical geological structure. The drainage density was calculated from the ALOS PALSAR DEM data by using spatial analyst extension inside ArcMap version 10.5. The study area classified into four classes and each class has given a weighted value which shows in table 1 and Fig.5 b. Generally, the value is ranged from less than 1 km/km^2 to 7 km/km^2.

3. Land use/ land cover map

Land use/land cover plays a significant role in the existence and alteration of groundwater present in the area, unless by decreasing runoff and promoting infiltration or impeding infiltration by increasing surface runoff. In the current study, LU/LC map is prepared using Landsat-8 images and ENVI 5.1 software. Accordingly, the study area divided into eight classes including cropland, forest, grassland, shrubland, wetland, water, impervious surface, and bare, Fig.5 c. Each class has a weighted value with representing priority effect on groundwater accumulation, Table 1.

4. Rainfall map

Precipitation is one of the most parameters which influence the amount of water that income to the basin area. The annual rainfall in the region is distribution differently started from October to May it is exceptional to have rainfall between June and September. The precipitation increases from SW to NE geographically. Due to the lack of metrological data for the nearby study area, a spatial rainfall map is created based on data obtained from international satellite GPM (global precipitation measurement) that provides accurate precipitation data which use to create rainfall distribution map [41]. The interval data of GPM for the period of 2014-2018 interval is used, the area classified to six categories of rainfall start from (622-750 mm/year) with interval 25 mm and each class has a weighted value (Fig.5 d).

Table 1: Weights and classes of factors in AHP method

Criteria	Class	Ranking	Class weight (%)	Weight (%)
Hydrogeological unit	intergranular Aquifer	1	45	20
	fissured Aquifer	2	33	
	Karstic Aquifer	3	15	
	Aquitard	4	7	
Drainage density (km/km^2)	<1	1	47	5
	1.1-2	2	28	
	2.1-4	3	16	
	>4.1	4	10	
LU/LC	Cropland	2	19	8
	Forest	1	21	
	Grassland	4	14	
	Shrubland	3	16	
	Wetland	5	12	
	Water	5	12	
	Impervious surface	7	3	
	Bareland	6	4	
Rainfall (mm/year)	<625	6	4	25
	626-650	5	6	
	651-675	4	10	
	676-700	3	16	
	701-725	2	25	
	>726	1	38	
Slope(degrees)	<2.2	1	38	13
	2.3-4.1	2	25	
	4.2-8.5	3	16	
	8.6-16	4	10	
	17-24	5	6	
	>25	6	4	
Soil type	C3	1	53	10
	C2.1	2	33	
	B2	3	14	
Topography (m)	<500	5	6	4
	501-1000	4	10	
	1001-1500	3	16	
	1501-2000	2	26	
	>2001	1	42	
Lineament (km/km^2)	<0.2	5	6	15
	0.21-0.4	4	10	
	0.41-0.6	3	16	
	0.61-0.8	2	26	
	>0.8	1	42	

5. Slope map

The slope map derived from ALOS PALSAR DEM using ArcGIS. The study area is classified into five classes depending on the slope variety. The areas arranging from (0-2.2) ° slope are considered as (very good) because of the flat terrain and relatively decreased runoff movement to downstream. The center part of the study area is mainly having (2.3-4.1,4.2-8.5) ° which considered as (good - moderate) are considered as favorable for groundwater recharge. The area between plain and mountain represents as (low-very low) which (8.6-16,17-24)° where infiltration occurs in a small amount. Those areas having a slope of more than 25 ° consider (very poor) due to the steep slope, which causes higher runoff. The slope map of the study area is demonstrated in Fig.6. a.

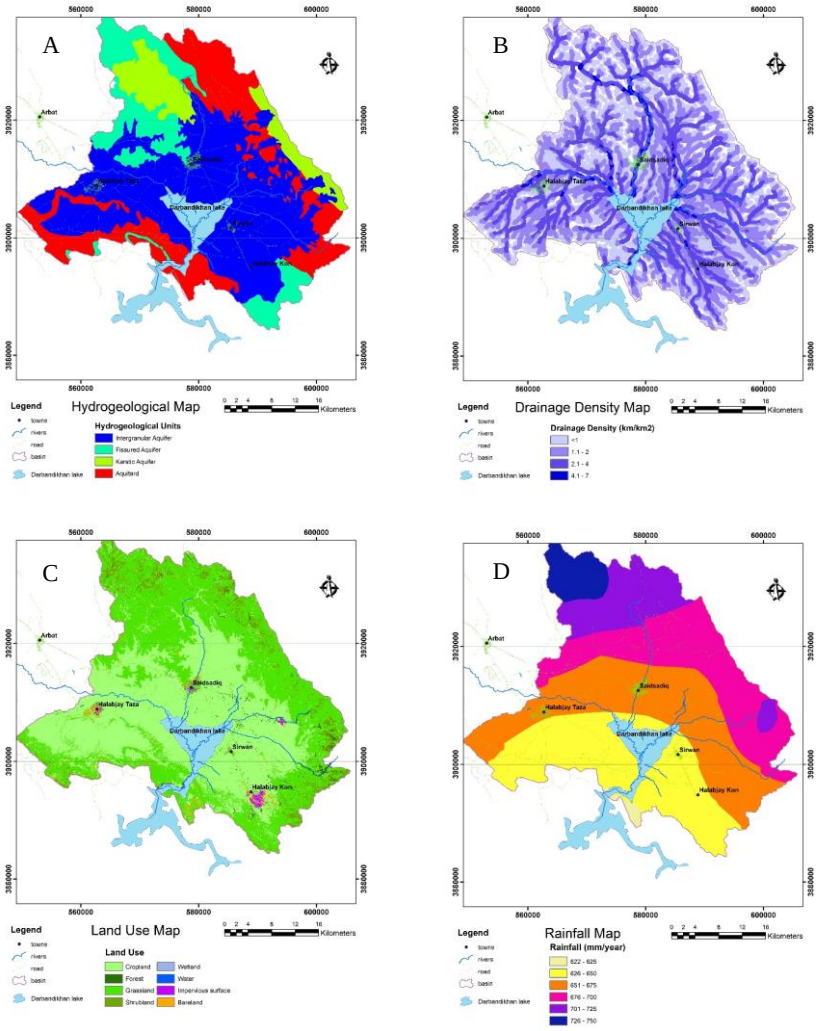

Fig. 5: A. Hydrogeological map B. Drainage density map C. LU/LC map D. Rainfall distribution map

6. Soil map

The soil has significant influences on the groundwater storage and infiltrations capacity because most of the study area covered by soil which is the first contact between precipitation and land. The study area is classified into three sets of soil Fig.6 b. The first soil type is (C3) deep well drained lime-rich non-gravely to gravelly silty clay to clay with surface cracks. With ranking (excellent) and also located in a very flat area in the basin. The second-ranking (good) gave to (C2.1) soil type, shallow to moderately deep well-drained loamy to clayey soil with variable gravel and stone content. The third-ranking (poor) gave to soil type (B2) shallow well-drained loamy to clayey soil with variable sand content in the rock outcrop area Fig.6 B.

7. Topography map

The topography map of the area was classified in to five classes according to elevation above sea level, the first class is < 500 m.a.s.l represents as (perfect);501-1000 represents as (very good); 1001-1500 represents as (good); 1501-2000 represent as (poor);>2000 represent as (very poor). The classification is done based on the correlation between elevation and shape features of the terrain by pairwise comparison which is favorable for the infiltration, Fig.6 C.

8. Lineament Density Map

The lineaments are increased secondary porosity and permeability and therefore of improved groundwater existence and movement [39]. A lineament distribution for the area extracted from Landsat 8 Thematic Mapper (TM) images, with cell size (30 × 30 m) resolution and nine spectral bands using PCI Geomatica (2016) software. The lineament density of the area has ranged from 0.2 km/km^2 to 1 km/km^2, Fig.6 D.

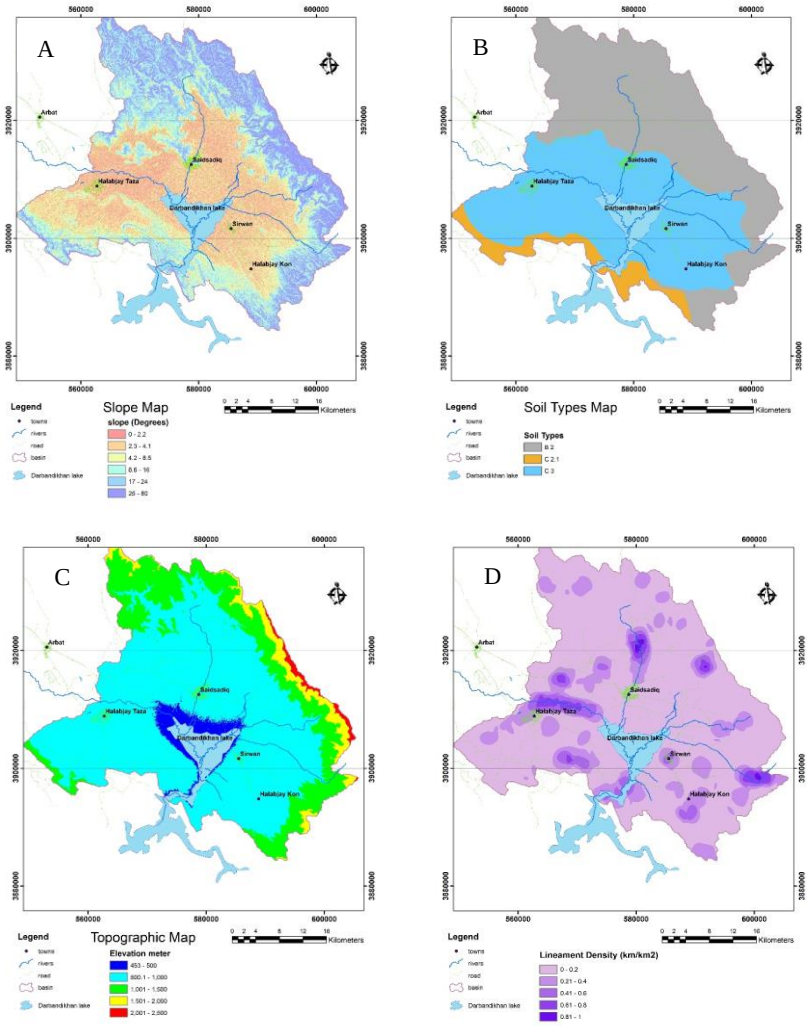

Fig. 6: A. Slope map B. Soil type map C. Topographic map D. Lineament density map.

Results and discussions

Geoelectrical resistivity and VES investigations

The results of the geoelectrical resistivity profiles are shown in Fig.7 & 8. The discussion below will be highlighted on the interpretation and analysis of the geoelectrical resistivity profiles.

The profile-1 is extending N45W, the first electrode plotted at SE end of the profile and electrode 72 at the NW ends as shown in Fig. (7a). Two distinguished zones have been identified; the first zone is represented by the blue color of low resistivity with respect to the second zone. The low resistivity of this zone is returned to disseminating of a large amount of clay with the fine silt. This layer composed of clay and silt cycle sedimentation of the recent sediments. It shows resistivity ranging from 8 Ωm to 28 Ωm. The second zone (green to redish color) is of high resistivity ranging from 40 to 1000 Ωm. It represents the limestone rocks of the Kometan Formation. The Limestone rocks are highly deformed and subjected to several faults forming horst and graben, they are detected at four locations which are, electrode 45 and at a depth equal to 64 m, electrode 53 and at a depth equal to 39 m, electrode 62 and at a depth equal to 20 m , and electrode 67 and at a depth equal to 20. The aquifer is observed from the depth 0 to 150, the Quaternary deposits extend to this depth below electrodes 1 to 30.

Profile-2 is running NW-SE, approximately parallel to the main strike of the outcrops. Three distinguished zones have been identified, Fig (7 b); the first zone represented by a thin layer covers the surface of the area has a thickness ranging from 1 to 20 m. it is of a wide range of resistivity from 14 to 70 Ωm, composed mainly of sandstone, siltstone, and clay. The second layer is characterized by the existence of more clay and little sandstone. It shows resistivity ranging from 7 Ωm to 12 Ωm. The thickness of this layer is ranging from 20 m to 45 m and extend to the maximum depth of investigation which equal to 86 m.The third layer shows high resistivity ranging from 20 to 60 Ωm, it is detected at a depths ranging from 35m to 150 m. This layer composed of the coarse material sandstone, siltstone, and little clay. It extends to the lower part of the resistivity section and to the maximum depth of investigation equal to 150 m, it represents the coarse material cycle of the recent sediments.

It is noticed that from the profile-3 that there are two distinguished zones; the first zone represented by the reddish color of high resistivity with respect to the second zone, the high resistivity of this zone is returned to disseminating of a large amount of sand and silt within the clay. It shows resistivity ranging from 27 Ωm to 80 Ωm (Fig.8a). The thickness of this layer is ranging from 20 m to 45 m. The second zone (green to blush color) is of low resistivity ranging from 10 to 25 Ωm, it represents clay and silt layers of the recent sediments. The Quaternary deposits extend to the maximum depth of investigation equal to 150 m.

The profile-4 is running NW-SE, approximately parallel to the main strike of the outcrops.Two distinguished zones have been identified, Fig. (8 b); the first zone represented by a layer covers the surface of the area has a thickness ranging from 20 to 65 m. it is of a wide range of resistivity from 20 to 95 Ωm, composed mainly of sandstone, siltstone, and clay. The second layer is characterized by the existence of more clay and little sandstone. It shows resistivity ranging from 7 Ωm to 17 Ωm. The thickness of this layer is ranging from 20 m to 150 meters and extend to the maximum depth of investigation which equal to 150 m.

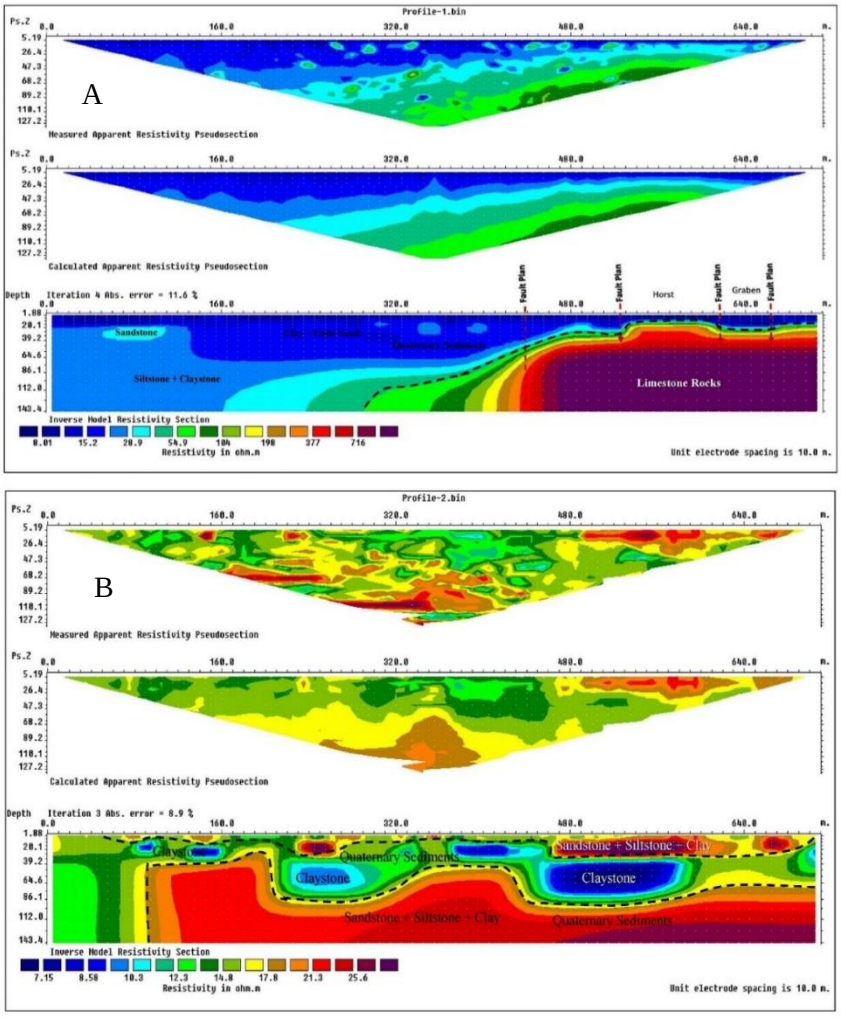

Fig. 7: Geoelectrical resistivity tomography model A. Profile- 1 B. Profile -2, Groundwater potential map based on AHP method

The output map of Groundwater potential in the study area is generated after assigning weights to all eight thematic maps and their attributes; the datasets are integrated into GIS using Equation (1). The groundwater potential model is created with the aid of Model Builder facility in the ArcGIS platform. The groundwater potential Models are workflows that chain together sequences of geoprocessing tools, providing the output of one tool into another tool as input. Model Builder can also be assumed as a visual programming language for building workflows [43].

$$GWPI = \sum_{j=1}^{m} \sum_{i=1}^{n} (wj * xi)$$

Where GWPI is Groundwater Potential Index, xi is the normalized weight of the *i*th class/feature of the theme, w*j* is the normalized weight of the *j*th theme, m is the total number of themes, and *n* is the total number of classes in a theme. All reclassified input layers were combined in GIS using raster calculation

techniques to produce the final groundwater potential map based on the weighted linear combination [44].
Groundwater potential map for the study area is categorized into three zones: low, moderate and high (Fig.9). Spatial distribution of these zones revealed that the first zone (low) is concentrated in the boundary of the basin at the north, east and south borders with 33% of the study area. The second zone (moderate) is desperate in many spots between low and high class with 24% of the study area. While the third zone (high) covering 43% of the study area, spatially located in the center of the basin where the intergranular aquifer is exposed in the study area and deserves to be concentrated for drilling and exploiting groundwater.

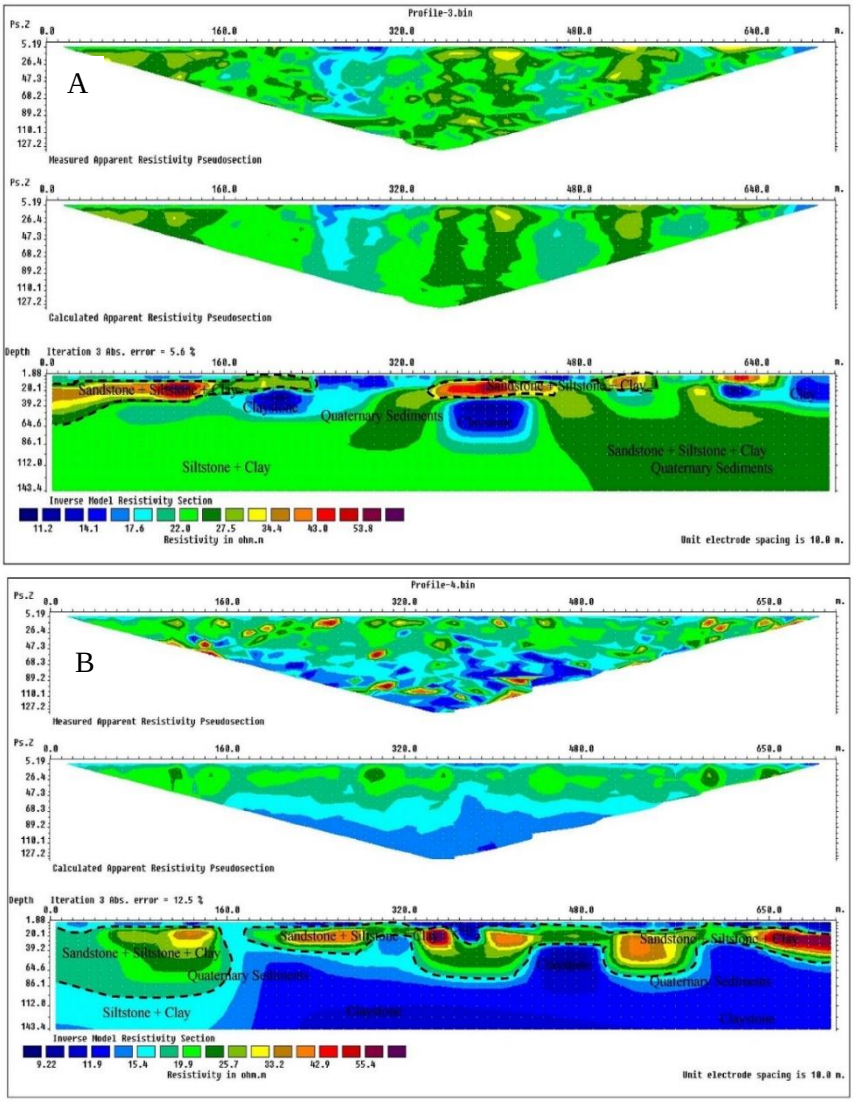

Fig. 8: Geoelectrical resistivity tomography model A. Profile- 3 B. Profile -4

Groundwater potential map verification

The groundwater potential zones consequently obtained were verified with well yield data of 580 wells that obtained from Sulaymaniyah Groundwater Directorate with depths ranging from 23 to 353 m with yield ranges from (0.2-22.5) l/s. The data of the wells in the study area were categorized into three categories which are good (>5 l/s), moderate (2– 5 l/s), and poor yield (<2 l/s) with (366,154,60) wells respectively.
The data also revealed that in high groundwater potential zone, which contains 440 wells, 67.5 % of wells are of good yield (>5 l/s) while 23.9 % of wells are of moderate yield (2–5 l/s) and 8.6% of wells are of poor yield (<2 l/s). In the moderate zone,117 wells located, 53.8 % of the wells are with good yield (>5 l/s), 33.3 % of the wells with moderate yield (2–5 l/s), and 12.8% of wells with poor yield (<2 l/s). In the low zone, there are 23 wells, 26.1 % of the wells are with good yield (>5 l/s), 43.5% of the wells with moderate yield (2–5 l/s), and 30.4 % of wells with poor yield (<2 l/s). The verification of groundwater potential zones shows that the model provides a guideline for designing an appropriate groundwater exploration strategy in the future. The spatial distribution of the several groundwater potential zones presents patterns of geology, lineaments, rainfall, topography, slope, soil, LU/LC, and

drainage. Spatially, the high category is distributed along Quaternary sediments with very high lineament density, depositional pediment, and low slope.

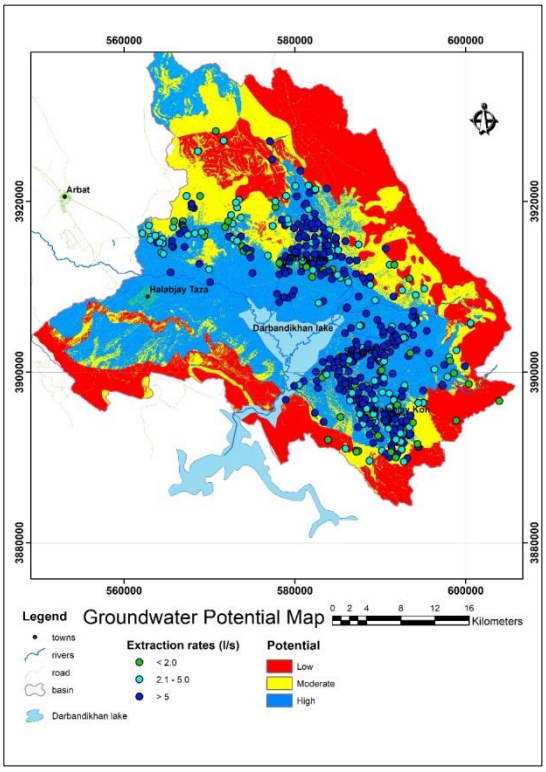

Fig. 9: Groundwater potential map and distribution of extraction wells of the study area.

Conclusions

In the present study, GIS platform and geophysical techniques have been used for delineating groundwater potential zones in Halabja Sais Sadiq sub- basin. modeling approach can be maximized for optimal exploration of groundwater resources in the study area the study focused on mapping various hydrogeological units, lineaments, drainage density, rainfall, slope, soil type, topography, and LU/LC. A combination of the two methods has shown that the groundwater potential zones focused within the Quaternary intergranular aquifer. The data of geoelectrical survey revealed that the thickness of the aquifer is more than 150 m. Hydrogeological and rainfall factors act as the most effective factors for determining groundwater potential zones.

Based on the results of the estimated GWPI, the study area was classified into three groundwater potential zones, low, moderate, and high. The zones coinciding with areas on Quaternary sediments within the study area. The medium and the high potential zones predicted in the area were compared with the geoelectrical profiles in the area.

Spatially, the low, medium and high groundwater potential zones cover 33 %, 24 %, and 43 %, respectively. In relation to field geology and geophysical investigation, areas of low potential and medium potential are characterized by karstified and fissured aquifers while zones of high groundwater potential are characterized by Intergranular aquifers. It is recommended that groundwater prospect mapping using GIS and geoelectrical resistivity be improved in helping the field geologists to quickly identify the groundwater potential zones.

Acknowledgments

The authors sincerely acknowledge Sulaymaniyah Groundwater Directorate for their kind and providing the needed wells data. The authors would like to thank Mr. Sarkhel H., Zana I., Assad I. for assisting in field data acquisition. Great appreciation goes to Professor Dr. Bakhtiar Q. for his guidance and valuable comments and the interpretation of geoelectrical profiles.

References

[1] Mogaji, K.A., Omosuyi, G.O., Adelusi, A.O. and Lim, H.S. (2016). Application of GIS-based evidential belief function model to regional groundwater recharge potential zones mapping in hardrock geologic terrain, *Environmental Processes. Springer*, **3(1)**: 93–123.

[2] Parameswari, K. and Padmini, T. K. (2018). Assessment of groundwater potential in Tirukalukundram block of southern Chennai Metropolitan Area, *Environment, development and sustainability*, **20(4)**: 1535–1552. https://doi.org/10.1007/s10668-017-9952-6.

[3] Jha, M. K., Chowdary, V. M., and Chowdhury, A. (2010). Groundwater assessment in Salboni Block, West Bengal (India) using remote sensing, geographical information system and multi-criteria decision analysis techniques. *Hydrogeology J*, **18(7)**:1713-1728.

[4] Al-Abadi, A. M., Al-Shamma'a, A. and others (2014). Groundwater potential mapping of the major aquifer in Northeastern Missan Governorate, South of Iraq by using analytical hierarchy process and GIS, *J Environ Earth Sci*, **10**:125–149.

[5] Al-Abadi, A. M. (2015). Modeling of groundwater productivity in northeastern Wasit Governorate, Iraq using frequency ratio and Shannon's entropy models, *Applied Water Science. Springer*, **7(2)**: 699–716. 10.1007/s13201- 015-0283-1.

[6] Minor, T. B., Carter, J. A., Chesley, M. M., Knowles, R. B., & Gustafsson, P. (1994). The use of GIS and remote sensing in groundwater exploration for developing countries (No. USATEC-R-236). Beloir, VA: Army Topographic Engineering Center Fort.

[7] Saraf, A. K. and Choudhury, P. R. (1998). Integrated remote sensing and GIS for groundwater exploration and identification of artificial recharge sites, *International journal of Remote sensing. Taylor & Francis*, **19(10)**:1825–1841.

[8] Chowdhury, A., Jha, M.K., Chowdary, V.M. and Mal, B.C. (2009). Integrated remote sensing and GIS-

based approach for assessing groundwater potential in West Medinipur district, West Bengal, India, *International Journal of Remote Sensing*, **30(1)**:231–250.
[9] Fashae, O.A., Tijani, M.N., Talabi, A.O. and Adedeji, O.I. (2014). Delineation of groundwater potential zones in the crystalline basement terrain of SW-Nigeria: an integrated GIS and remote sensing approach, *Applied Water Science*, **4(1)**:19–38.
[10] Krishnamurthy, J., Venkatesa Kumar, N., Jayaraman, V. and Manivel, M. (1996). An approach to demarcate ground water potential zones through remote sensing and a geographical information system, *International Journal of Remote Sensing*, **17(10)**: 1867–1884.
[11] Oh, H.J., Kim, Y.S., Choi, J.K., Park, E. and Lee, S. (2011). GIS mapping of regional probabilistic groundwater potential in the area of Pohang City, Korea, *Journal of Hydrology*, **399(3–4)**:158–172.
[12] Sonkamble, S., Satishkumar, V., Amarender, B. and Sethurama, S. (2014).Combined ground-penetrating radar (GPR) and electrical resistivity applications exploring groundwater potential zones in granitic terrain, *Arabian Journal of Geosciences*, **7(8)**: 3109–3117.
[13] Venkateswaran, S., Vijay Prabhu, M. and Karuppannan, S. (2014). Delineation of groundwater potential zones using geophysical and GIS techniques in the Sarabanga Sub Basin, Cauvery River, Tamil Nadu, India, *Int J Curr Res Acad Rev. Citeseer*, **2(1)**: 58–75.
[14] Al-Manmi, D. A. M. and Rauf, L. F. (2016). Groundwater potential mapping using remote sensing and GIS-based, in Halabja City, Kurdistan, Iraq, *Arabian Journal of Geosciences*, **9(5)**. doi: 10.1007/s12517-016-2385-y.
[15] Mohammed, S. . (2017). Groundwater Potential Mapping using Remote Sensing and GIS of a part of Chamchamal basin, Sulaimani, Kurdistan region, Iraq, M.Sc. thesis, University of Miskolc, Hungary:70 pp.
[16] Islami, N., Taib, S.H., Yusoff, I. and Ghani, A.A. (2018). Integrated geoelectrical resistivity and hydrogeochemical methods for delineating and mapping heavy metal zone in aquifer system, *Environmental Earth Sciences*, **77(10)**:383. doi: 10.1007/s12665-018-7574-4.
[17] Hussain, H. Musa, Ahmed H. Jawad, (2008). Assessment of Groundwater Potential in Western Desert of Iraq Using GIS, Proceedings of The First Conference for Pure & Applied Sciences, 12-13 Mar 2008, Kufa, Iraq, University of Kufa: p. 247 – 262.
[18] Al-Abadi A.M. (2011). Hydrological and Hydrogeological Analysis of Northeast Missan Governorate, South of Iraq Using Geographic Information System, Ph.D. thesis, University of Baghdad, Baghdad, Iraq: 220 pp.
[19] Kowalsky, M.B., Gasperikova, E., Finsterle, S., Watson, D., Baker, G. and Hubbard, S.S. (2011). Coupled modeling of hydrogeochemical and electrical resistivity data for exploring the impact of recharge on subsurface contamination, *Water Resources Research. Wiley Online Library*, **47(2)**.
[20] Hago, H. A. (2000). Application of Electrical Resistivity Methods in Quantitative Assessment of Groundwater Reserve of Unconfined Aquifer. Universiti Putra Malaysia: 191 pp.
[21] Ndatuwong, L. G. and Yadav, G. S. (2015). Application of geoelectrical data to evaluate groundwater potential zone and assessment of overburden protective capacity in part of Sonebhadra district, Uttar Pradesh, *Environmental earth sciences*, **73(7)**: 3655–3664.
[22] Talen, E. and Shah, S. (2007). Neighborhood evaluation using GIS: An exploratory study, *Environment and Behavior*. Sage Publications Sage CA: Los Angeles, CA, **39(5)**: 583–615.
[23] Arkoprovo, B., Adarsa, J. and Prakash, S. S. (2012). Delineation of groundwater potential zones using satellite remote sensing and geographic information system techniques: a case study from Ganjam district, Orissa, *India*. **1(9)**:59-66.
[24] Prakash, S. R., & Mishra, D. (2013). Identification of groundwater prospective zones by using remote sensing and geoelectrical methods in and around Saidnagar area, Dakor block, Jalaun district, U.P. *Journal of the Indian society Remote sensing*, **21(4)**:217–227.
[25] Kumar, S. S., Arivazhagan, S. and Rangarajan, N. (2013). Remote Sensing and GIS Applications in Environmental Sciences--A Review, *Journal of Environmental and Nanotechnology*. **2 (2)**: 92-101.
[26] The Regional Geology of Iraq, Vol. I. Stratigraphy and Paleogeography. I.I.M. Kassab and S.Z. Jassim (eds.). SOM, Baghdad, Dar El Kutib Publ. House, University of Mosul: 445pp.
[27] Buday, T. and Jassim, S. Z. (1987). The regional geology of Iraq, vol. 2, Tectonism, Magmatism and Metamorphism, Publication of GEOSURV, Baghdad: 352 pp.
[28] Bellen R.C., Dunnington H.V., Wetzel R., and Morton D. (1959). Lexique Stratigraphique International: Asie. *Iraq. Tertiary. Mesozoic and Palaeozoic*. Centre National de la Recherche Scientifique: 333 pp.
[29] Ali, S. S. (2007). Geology and hydrogeology of Sharazoor-Piramagroon basin in Sulaimani area, northeastern Iraq, Ph.D desertation, Faculty of Mining and Geology. University of Belgrade, Belgrade, Serbia: 330 pp.
[30] Telford, W.M., Telford, W.M., Geldart, L.P., Sheriff, R.E. and Sheriff, R.E. (1990) Applied geophysics. Cambridge University press: 792 pp.
[31] Aziz, B. Q. (2005). Two dimension resistivity imaging tomography for hydrogeological study in Bazian basin, west Sulaimani city, NE-Iraq, Unpublished Ph.D. thesis, University of Sulaimani, Sulaymaniyah, Iraq: 183 pp.
[32] Loke, M. H. and Barker, R. D. (1996). Rapid least-squares inversion of apparent resistivity

pseudosections by a quasi-Newton method 1, *Geophysical prospecting. Wiley Online Library*, **44(1)**: 131–152.
[33] Loke, M. H. (2007). Rapid 2-D Resistivity and IP inversion using the least-squares method, Geoelectrical Imaging 2D and 3D. GEOTOMO SOFTWARE, Malaysia.
[34] Saaty, T. L. (1990). An exposition of the AHP in reply to the paper remarks on the analytic hierarchy process, Management science. *INFORMS*, **36(3)**: 259–268.
[35] Saaty, T. L. and Vargas, L. G. (2012). Models, methods, concepts & applications of the analytic hierarchy process. Springer Science & Business Media: 343 pp.
[36] Agarwal, R. and Garg, P. K. (2016). Remote sensing and GIS based groundwater potential & recharge zones mapping using multi-criteria decision making technique, *Water resources management*, **30(1)**: 243–260. https://doi.org/10.1007/s11269-015-1159-8.
[37] Dadgar, M.A., Zeaieanfirouzabadi, P., Dashti, M. and Porhemmat, R. (2017). Extracting of prospective groundwater potential zones using remote sensing data, GIS, and a probabilistic approach in Bojnourd basin, NE of Iran, *Arabian Journal of Geosciences*, **10(5)**: 14. https://doi.org/10.1007/s12517-017-2910-7
[38] Chuma, C., Orimoogunje, O.I.O., Hlatywayo, D.J. and Akinyede, J.O. (2013). Application of Remote Sensing and Geographical Information Systems in Determining the Groundwater Potential in the Crystalline Basement of Bulawayo Metropolitan Area, Zimbabwe, *Advances in Remote Sensing*, **2(02)**: 149–161. doi: 10.4236/ars.2013.22019.
[39] Lemacha, G. (2008). Groundwater potential for upper Tumet catchment, Merge and Komosha woredas, Benishangul-Gumuz region, Guide for GIS developers, WaterAid Ethiopia and Ripple www. rippleethiopia. org.
[40] Adeyeye, O. A., Ikpokonte, E. A. and Arabi, S. A. (2018). GIS-based groundwater potential mapping within Dengi area, North Central Nigeria, *The Egyptian Journal of Remote Sensing and Space Science*. Elsevier, in press, https://doi.org/10.1016/j.ejrs.2018.04.003.
[41] Abdullah, T. (2018). Groundwater vulnerability mapping and Environmental studies of Halabja- Said SadiqBasin, Sulaimani, North East/ Iraq. Ph.D. thesis, College of Science, University of Sulaimani, Sulaymaniyah, Iraq: 236 pp.
[42] Acker, J. G. and Leptoukh, G. (2007). Online analysis enhances use of NASA earth science data, *Eos, Transactions American Geophysical Union*. Wiley Online Library, **88(2)**, pp. 14–17.
[43] Bruse, M. and others (2015). ENVI-met, *Available online: www. envi-met. com/(accessed on 1 June 2017)*.
[44] Malczewski, J. (1999). GIS and multicritxxeria decision analysis. John Wiley & Sons: 408 pp.

تكامل التقنيات المعتمدة على نظم المعلومات الجغرافية والتحريات الجيوفيزيائية لتقييم وفرة المياه الجوفية في حوض حلبجة سيد صادق، كردستان، شمال شرق العراق

هاوبير عطا كريم ، دياري علي محمد امين المنمي

كلية العلوم ، جامعة السليمانية

الملخص

تعتبر المياه الجوفية موردا هاما في حوض حلبجة سيد صادق، منطقة السليمانية للاستخدامات الزراعية وغيرها. أدى الاستخراج الجائرو المستمر للمياه الجوفية من الآبار المرخصة وغير المرخصة إلى انخفاض حاد في منسوب المياه على مدى ثلاثين سنة الماضية. تتمثل أهداف هذه الدراسة في تحديد مناطق إنتاجية المياه الجوفية من خلال الجمع بين نظم المعلومات الجغرافية والمسح الجيوكهربائي، والذي يعمل على التعرف على مواقع مناطق تخزين وتغذية المياه الجوفية الجيدة. تم اختيار حوض حلبجة سيد صادق كدراسة حالة لتحديد مناطق إنتاجية المياه الجوفية. تم اخذ أربعة مقاطع المقاومة الجيوكهربائية مع تباعد القطب 10 م وطول المقطع كان 710 م. يتم استخدام معلومات مثل الهيدروجيولوجيا، واستخدام الأرض / غطاء الأرض، والطوبوغرافيا، وكثافة الصرف، ونوع التربة، والمنحدر، والنسب وخرائط هطول الأمطار. تم وضع الخرائط الموضوعية المصممة باستخدام نظام GIS الأساسي والأوزان المناسبة على السمات مع مراعاة التأثير على إمكانية تخزين المياه الجوفية. كشفت نتائج المقاطع الجيوكهربائية أن سمك طبقة المياه الجوفية يبلغ 150 متراً. ثلاث مناطق من وفرة المياه الجوفية المحددة والتي هي منخفضة ومعتدلة وعالية وتغطي 33 ٪، 24 ٪، و 43 ٪ من المساحة الكلية على التوالي. من الناحية المكانية، تقع أعلى منطقة جنبًا إلى جنب مع الرواسب الرباعية التي تتميز بالكثافة العالية للنسب، والانحدار المنخفض، والپيديمنت.

تم التحقق من نتائج نموذج وفرة المياه الجوفية من خلال اختبار معدل تصريف الآبار الحالية البالغ عددها 580 بئراً. أظهرت النتائج أن معظم الآبار عالية العطاء تقع داخل نطاق وفرة المياه الجوفية العالي. أثبتت نتائج عمليات التحقق هذه أن مناطق إنتاجية المياه الجوفية المحددة من خلال نظم المعلومات الجغرافية (AHP) (GIS) والتقنيات الجيوكهربائية الجوفية يمكن الاعتماد عليها وعملية.